

Fermi National Accelerator Laboratory

FN-485

Coherent Betatron Instability in a High Energy Synchrotron*

S. A. Bogacz, M. Harrison, and K.-Y. Ng
Accelerator Theory Department
Fermi National Accelerator Laboratory
P.O. Box 500, Batavia, Illinois 60510

May 1988

*Submitted to Phys. Rev. D



Operated by Universities Research Association Inc. under contract with the United States Department of Energy

COHERENT BETATRON INSTABILITY IN A HIGH ENERGY SYNCHROTRON[†]

S.A. Bogacz, M.Harrison and K.Y. Ng

Accelerator Theory Department, Fermi National Accelerator Laboratory*, P.O. Box 500,
Batavia, IL 60510, USA

May 1988

ABSTRACT

Presented study is motivated by a coherent betatron instability observed in the Tevatron. The instability, which develops rapidly just before the "flat top" (> 600 GeV) is characterized by the growth-times of $30-50 \times 10^{-3}$ sec and the horizontal amplitude of about 2 mm. A simple analytic study based on the Sacherer's formalism, assuming the so-called 'plane wave' model of the transverse modes allowed to link different growth-time scales with the specific contributions to the transverse coupling impedance. The observed instability was identified as a combination of low frequency resistive wall component and a single bunch $l = 1$ head-tail mode driven by the transverse impedance of the kicker magnets. This result is in close agreement with the experimental data and the same calculation done in the framework of a more realistic Vlasov equation-based 'air bag' model. Some guidance about damping of specific modes is provided by the chromaticity dependence of the calculated growth-rates. Another possible cure involving Landau damping through the octupole-induced tune spread is also addressed. Finally, a closed form of the growth time vs chromaticity was obtained analytically in the case of the slow head-tail instability driven by the transverse impedance of the kicker magnets.

[†] Paper submitted to Phys. Rev. D

* Operated by the Universities Research Association under contract with the U.S. Department of Energy

INTRODUCTION - BEAM INSTABILITY OBSERVATIONS

The instability was first observed during the recent 1987-88 Tevatron fixed target run. In this operating mode 1000 consecutive bunches are loaded into the machine at 150 GeV with a bunch spacing of 18.8×10^{-9} sec (53 MHz). The normalized transverse emittance is typically $15 \pi \times 10^{-6}$ m rad in each plane with a longitudinal emittance of about 1.5 eV-sec. The beam is accelerated to 800 GeV in 13 sec. and then it is resonantly extracted during a 23 sec flat top. As the run progressed the bunch intensities were increased until at about 1.4×10^{10} ppb (protons per bunch) we experienced the onset of a coherent horizontal oscillation taking place in the later stages of the acceleration cycle (> 600 GeV). This rapidly developing coherent instability results in a significant emittance growth, which limits machine performance and in a catastrophic scenario it even prevents extraction of the beam.

The characteristics of the instability are as follows: It was only observed in the horizontal plane and at the higher energies, we were unable to detect any obvious longitudinal modes. There was a relatively strong intensity threshold; 10% changes in bunch intensity would completely eliminate the effect. The oscillation was self-stabilizing at the 2-3 mm betatron amplitude level. The effect was non-resonant with no strong dependence on the tune. The intensity threshold could be increased by reducing the chromaticity to be positive but close to zero (1-2 units) but there was no dramatic sensitivity to chromaticity.

The most successful method of raising the intensity threshold was achieved by increasing the longitudinal emittance by applying white noise to the rf drive, an emittance of 5 eV-sec. would permit a bunch intensity of about 1.8×10^{10} ppb. The growth time was fast; less than 30×10^{-3} sec. Typically, the full ring would go unstable, but we have observed unstable behavior in a partial azimuth of the ring when bunches of significantly higher intensity were present. Attempts at Landau damping with

octupole circuits had no great effect but our ability to do this was hampered by the fact that the value of the octupoles at flattop was constrained by the resonant extraction process.

The instability was characterized by a strong low frequency signal at the first betatron sideband of the revolution frequency (~ 25 kHz). This is shown in Fig.1, which is the output from a beam position monitor showing the beam position over 10 turns. The tick marks represent the gap in the circulating beam, which is coming once per revolution. Using a wide band pickup (2 GHz) we attempted to identify any higher frequency components such as those expected from intrabeam oscillations. While these measurements are difficult to make, we were unable to see any strong evidence for higher order modes within the bunches, which we would have expected in the 500 – 900 MHz region.

In the next few sections, we will present a simple analytic description of the observed instability. We will show that a combination of a resistive wall coupled bunch effect and a single bunch slow head-tail instability is consistent with the above observations. Finally, a systematic numerical analysis of our model (growth-time vs chromaticity plots) points to the existence of the $\ell \geq 1$ slow head-tail modes as a plausible mechanism for the observed coherent instability. This last claim, as mentioned before, does not have conclusive experimental evidence, although it is based on a very good agreement between the measured values of the instability growth-time and the ones calculated on the basis of our model.

1. COHERENT BETATRON INSTABILITY - STANDING WAVE MODEL

We consider a case where both longitudinal and transverse oscillations are coupled through a finite chromaticity, ξ , according to the following relationship

$$\Delta\nu = \xi \frac{\Delta p}{p}. \quad (1.1)$$

Here $\Delta\nu$ is the betatron tune shift and Δp is the longitudinal momentum deviation measured with respect to the synchronous particle (Δp defines position of a given particle within the bunch). One can consider a single particle initially at the "head" of the bunch ($\Delta p = 0$); its betatron tune matches the one of the synchronous particle. We also assume that both particles have initially the same betatron phases. Since the particle is undergoing synchrotron oscillations, while it is moving towards the "tail" of the bunch it lags in the betatron phase behind the synchronous particle ($\Delta\nu < 0$). After half of the synchrotron period the phase lag, χ , reaches maximum and the particle continues moving back towards the "head" of the bunch regaining previously lost phase. When a full synchrotron oscillation is completed the initial phase matching is recovered.

One can simply express the accumulated phase-lag in terms of the arrival time off-set, τ , (measured with respect to the synchronous particle) as follows

$$\chi = \frac{\xi}{\eta} \omega_0 \tau, \quad (1.2)$$

where ω_0 is the revolution frequency and η is the frequency dispersion function ($\eta < 0$ below the transition). Following an intuitive model of the head-tail instability proposed by Sacherer¹ we will assume that the amplitude of the transverse beam oscillation (related to the pick-up monitor signal) is a superposition of a standing plane wave (with the number of internal nodes defining the longitudinal mode index l) and a propagating

part describing previously discussed betatron phase lag/gain process (due to the finite chromaticity). The amplitude signal can be written as

$$A_{\ell}(\tau, k) = P_{\ell}(\tau) e^{i\omega_{\xi}\tau + 2\pi i k v} , \quad (1.3)$$

where $\omega_{\xi} = \frac{\xi}{\eta} \omega_0$ and k denotes the revolution number. Here the standing wave profile is modelled by simple harmonic functions

$$P_{\ell}(\tau) = \begin{cases} \cos[(\ell + 1) \pi \tau / 2\hat{\tau}] & \ell \text{ even} \\ \sin[(\ell + 1) \pi \tau / 2\hat{\tau}] & \ell \text{ odd} \end{cases} , \quad (1.4)$$

where $2\hat{\tau}$ is the bunch length (in units of time). Assuming small amplitude (harmonic) synchrotron motion, $\hat{\tau}$ is given by the following expression

$$\hat{\tau} = \sqrt[4]{\frac{2\varepsilon^2\eta}{\pi\omega_0^2 E_0 \gamma e \hat{V} \cos\phi_s}} . \quad (1.5)$$

Here ε is the longitudinal emittance (eV-sec), E_0 is the rest energy of a proton, \hat{V} is the amplitude of the rf voltage, ϕ_s is the synchronous phase and γ is the Lorentz contraction factor.

One can easily find the power spectrum of the transverse beam signal by taking the Fourier transform of Eq.(1.3)

$$A_{\ell}(\omega, k) = P_{\ell}(\omega - \omega_{\xi}) e^{2\pi i k v} \quad (1.6)$$

where

$$P_{\ell}(\omega) = \mathcal{F}\{P_{\ell}(\tau)\}$$

One can see, that the beam spectrum is shifted by ω_ξ due to the presence of the propagating wave component. Periodicity given by the revolution period, $2\pi/\omega_0$, yields the discrete frequency spectrum with spacing ω_0 . The envelope of the power spectrum is defined as

$$h_\ell(\omega) = |P_\ell(\omega)|^2$$

and is sampled by the frequencies (1.7)

$$\omega_p = (p + \nu)\omega_0$$

where p is an integer.

The explicit form of the power spectrum is given by the following expression

$$h_\ell(\omega) = \frac{4}{\pi^2} (\ell + 1) \frac{1 + (-1)^\ell \cos(2\omega\hat{t})}{|(2\omega\hat{t}/\pi)^2 - (\ell + 1)^2|^2} , \quad (1.8)$$

which will serve as a spectral density function in evaluation of the averaged transverse self-force driving specific slow head-tail modes.

2. SINGLE PARTICLE EQUATION OF MOTION - GROWTH TIME

Following Sacherer's argument¹ one can generalize a simple equation of motion describing a wake field driven coherent betatron motion of a coasting beam to model the head-tail instability of the bunched beam. A simple dipole oscillation of the coasting beam as a whole is governed by the following equation

$$\ddot{x} + (v\omega_0)^2 x = i \frac{e\beta}{\gamma m_0} \frac{Z_{\perp} I}{2\pi R} x . \quad (2.1)$$

Here x is the transverse displacement, Z_{\perp} denotes the transverse coupling impedance, I is the total beam current and R is the machine radius. The following approach assumes ad hoc existence of a given head-tail mode, ℓ , previously described by Eqs.(1.3) and (1.4), by imposing specific periodic dependence of the betatron motion with respect to the longitudinal position, τ . This dependence is given by the following formula

$$x^{\ell}(t, \tau) = e^{i\Omega_{\ell} t} \sum_{p=-\infty}^{\infty} x_p^{\ell} \exp(i\pi(\ell+1)p\tau/2\hat{\tau}) , \quad (2.2)$$

where Ω_{ℓ} is the coherent frequency. The above expression imposes $(\ell+1)$ -fold periodicity on the betatron amplitude along the bunch.

In a case of a bunched beam the wake field experienced by a test particle at the position τ is now given by the following convolution of the transverse impedance and the normalized beam spectrum, ρ

$$V^{\ell}(\tau) = \omega_0 \sum_{p=-\infty}^{\infty} Z_{\perp}(\omega_p) \rho^{\ell}(\omega_p - \omega_{\xi}) e^{i\omega_0 \tau p} . \quad (2.3)$$

where the beam spectrum for a given mode is defined as follows

$$\rho^l(\omega) = \frac{h^l(\omega)}{\sum_{p=-\infty}^{\infty} h^l(\omega_p)} . \quad (2.4)$$

The deflecting transverse wake force acting on the particle is a sum of the wakes generated by all the particles in the bunch, which are ahead of the test particle (causality); it also includes long range wakes left from all the preceding turns. The last feature is explicitly built into the definition of $V^l(\tau)$, given by Eq.(2.3). Resulting transverse wake force is conveniently expressed by the following integral

$$F^l(\tau) = i \frac{e\beta}{\gamma m_0} \frac{I_0}{2\hat{\tau}c} \int_{\tau}^{\hat{\tau}} d\tau' V^l(\tau') h^l(\tau') . \quad (2.5)$$

Substituting the above expression in the RHS of Eq.(2.1) and replacing x by Eq.(2.2) one obtains a complete equation of motion for the l -th head-tail mode. Applying the following orthogonality identity

$$\frac{1}{2\hat{\tau}} \int_{-\hat{\tau}}^{\hat{\tau}} d\tau' \exp(\pi(l+1)(p-p')\tau'/2\hat{\tau}) = (l+1) \delta_{p',p} , \quad (2.6)$$

one can carry out the integration in Eq.(2.5). The resulting decoupled equation of motion for a single Fourier component is given by

$$[(v\omega_0)^2 - \Omega_l^2 - i \frac{e\beta}{\gamma m_0} \frac{I_0}{2\hat{\tau}c} \frac{1}{l+1} \sum_{p'=-\infty}^{\infty} Z_{\perp}(\omega_{p'}) \rho^l(\omega_{p'} - \omega_{\xi})] \mathbf{x}_p^l = 0 . \quad (2.7)$$

Assuming a nontrivial solution for x_p^ℓ yields explicit formula defining coherent frequency of the ℓ -th mode. Its imaginary part (with the negative sign) represents the inverse growth-time and is expressed by the following formula

$$\frac{1}{\tau^\ell} = -\frac{ce\beta I_0}{4\pi E v} \operatorname{Re} Z_{\text{eff}}^\ell, \quad (2.8)$$

where $E = \gamma m_0 c^2$ is the total energy and Z_{eff}^ℓ is the effective impedance defined as follows

$$Z_{\text{eff}}^\ell = \frac{2\pi}{\ell + 1} \frac{1}{2\omega_0 \hat{\tau}} \sum_{p'=-\infty}^{\infty} Z_\perp(\omega_{p'}) \rho^\ell(\omega_{p'} - \omega_\xi) \quad (2.9)$$

The above result can be compared with the growth-time obtained in the framework of the Vlasov equation-based description of the slow head-tail instability. The so-called "air bag" model² assumes δ -like shell structure of the longitudinal phase-space, which serves as the equilibrium density distribution function (on top of which various head-tail modes are constructed as small fluctuations of the particle density). The resulting formula has exactly the same generic form as given by Eq.(2.8) with the effective impedance introduced as an average over different set of spectral density functions; namely the Bessel functions of the first kind. This average is given explicitly as follows

$$Z_{\text{eff}}^\ell = \sum_{p'=-\infty}^{\infty} Z_\perp(\omega_{p'}) J_\ell^2((\omega_{p'} - \omega_\xi) \hat{\tau}). \quad (2.10)$$

To remove model dependence from our study both results will be applied to carry out model calculation of the specific head-tail instability in the Tevatron. The results of the next sections show clearly that there is very little difference between both models.

3. TRANSVERSE COUPLING IMPEDANCE

Our consideration will be confined to the real part of the impedance only, since the imaginary part does not enter explicitly into the growth-time formulae given by Eqs.(2.8) and (2.9). We tentatively identified four dominant sources of the transverse impedance. These potentially offending vacuum structures can be listed as follows

- (a) bellows
- (b) kicker magnets
- (c) beam position monitors
- (d) resistive wall and Lambertson magnet laminations.

(a) The first contribution was estimated numerically using the TBCI code (real time solution of the Maxwell equations for a given geometry excited by a Gaussian test bunch). Calculated Fourier transform of the transverse wake field is translated into the transverse impedance in Ohm/m and is illustrated in Fig.2. The solution can be fitted into a broad-band resonance parametrized by the shunt impedance R_{sh} , the quality factor Q and the resonant frequency ω_c . The resulting fit is summarized by

$$Z_{\perp}(\omega) = \frac{R_{sh} \omega / \omega_c}{1 + iQ(\omega / \omega_c - \omega_c / \omega)} , \quad (3.1)$$

where

$$R_{sh} = 1.2 \times 10^6 \text{ Ohm/m}$$

$$Q = 3.3$$

$$\omega_c = 2\pi \times 9.1 \text{ GHz.}$$

(b) There are eleven kicker magnets; both injection and abort kickers located around the ring. According to Ref.3 the real part of the transverse coupling impedance of a c-magnet of half-width a , half-height b and length L is given by the following analytic expression

$$\text{Re } Z_{\perp}(\omega) = \frac{Z_0 L}{4ab} \frac{1}{\omega} \left(1 - \cos \frac{\omega L}{c}\right) , \quad (3.2)$$

where

$$Z_0 = 377 \text{ Ohm}$$

$$L = 1 \text{ m}$$

$$a = 3.7 \text{ cm}$$

$$b = 1.9 \text{ cm.}$$

(c) Similar contribution comes from 108 beam position monitors. Each unit consists of a pair of cylindrical strips of length l and width $b\phi_0$ forming a simple transmission line of the characteristic impedance Z_s . The real part of the transverse impedance is expressed as follows³

$$\text{Re } Z_{\perp}(\omega) = \frac{8Z_s}{\pi^2 b^2} \frac{c}{\omega} \sin^2 \frac{\phi_0}{2} \sin^2 \frac{\omega l}{c} , \quad (3.3)$$

where

$$l = 18 \text{ cm}$$

$$Z_s = 50 \text{ Ohm}$$

$$b = 3.5 \text{ cm}$$

$$\phi_0 = 1.92 \text{ rad.}$$

(d) Finally, the low frequency contribution to the transverse impedance due to the resistive wall and Lambertson magnet laminations is given by the following standard expression⁴

$$Z_{\perp}(\omega) = (1 + i) \frac{W}{\omega/\omega_0} , \quad (3.4)$$

where

$$W = 2.3 \times 10^6 \text{ Ohm/m.}$$

All four contributions will serve as a starting point for calculation of the effective impedance which will be carried out in the next section.

4. EFFECTIVE IMPEDANCE - GROWTH TIME

In order to evaluate the effective impedance one has to convolute the above four contributions to the transverse impedance with the beam spectrum according to Eqs.(2.9) and (2.10). Several lower harmonics of the beam spectrum are illustrated in Fig.3. The result of the above summation obviously depends on chromaticity. The resistive wall contributes only one term; either evaluated at $\nu\omega_0$ or at $(1 - \nu)\omega_0$. This is a consequence of the fact that for any neighboring sampling frequency the transverse impedance is negligibly small (hyperbolic tail). Therefore, only one spectral line at very low frequency (~ 25 kHz) couples to the resistive wall impedance causing existence of the stationary long range pattern depicted in Fig.4. Coherent motion of individual bunches is coupled due to the presence of long range wake field which leads to this low frequency correlation of the betatron amplitudes defining transverse motion of the bunch centroids⁴.

One can notice that for both contributions (b) and (c) their transverse impedances $Z_{\perp}(\omega)$, given by Eqs.(3.2) and (3.3), have a diffraction-like character; a principle maximum of width $\lambda = \pi c/L$ at the origin and a series of equally spaced secondary maxima governed by the same width. Similarly, the harmonics of the beam spectrum, $\rho^{(\ell)}(\omega - \omega_{\xi})$, have one ($\ell = 0$) or a pair ($\ell \geq 1$) of principle maxima of width $\varepsilon = \pi/2\hat{\tau}$ followed by a sequence of secondary maxima (See Fig.3). Both spectra are sampled by a discrete set of frequencies, $\omega_p = (p + \nu)\omega_0$. In case of relatively long proton bunches in the Tevatron at 800 GeV ($2\hat{\tau} = 2 - 3 \times 10^{-9}$ sec) both widths λ and ε are comparable and they are of the order of the chromatic frequency, ω_{ξ} , evaluated at about 10 units of chromaticity. These features combined with the convolution formula for the effective impedance, Eqs.(2.9) and (2.10), result in substantial 'overlap' of the transverse impedance and the beam spectrum, which in turn leads to large values of effective impedance for relatively small chromaticities ($\xi \sim 10$).

In contrast, the effective impedance evaluated with the broad-band part (a) of the transverse impedance is much smaller than the previously discussed one. The last statement can be explained as follows; the width of the broad-band impedance peak, $\delta = \omega_c/Q$, is much larger than ϵ and in order to overlap this broad peak with the principal maximum of the power spectrum harmonics (to get a nonzero effective impedance) one would have to shift both spectra by ω_ξ of the order of δ . This, in turn, would require enormous values of the chromaticity ($\xi \sim 10^4$).

Summarizing, only two out of four contributions to the transverse impedance are relevant to the discussed coherent betatron instability. First, the resistive wall part, which couples to the low frequency (~ 25 kHz) single spectral line is responsible for the observed coupled bunch pattern. Second, the kicker magnet contribution driving high frequency band of several lines centered around 500 MHz is in turn responsible for single bunch slow head-tail modes. The similar coupling due to the beam position monitors is much weaker, because of the small absolute value of the transverse impedance and therefore is neglected in further consideration. A closed analytic expression for the inverse growth-time of the slow head-tail modes, ℓ , driven by the kicker magnet impedance only is derived in detail in the Appendix.

5. CONCLUSIONS

At this point some the comparison of numerically evaluated results of the presented model with the observed coherent instability is in order. Assuming only two dominant contributions to the transverse coupling impedance; resistive wall given by Eq.(3.4) and kicker magnets expressed by Eq.(3.2), the inverse growth-time was calculated numerically according to Eqs.(2.8)–(2.10). The resulting growth-rate as a function of chromaticity evaluated for different slow head-tail modes ($l = 0, 1, 2, 3$) are illustrated in Fig.5. One can immediately see a qualitative difference between the $l = 0$ and $l > 1$ modes; the resistive wall effect is much more dramatic for $l = 0$ mode and leads to strong instability even at zero chromaticity. Higher order modes, on the other hand, are only slightly effected by the resistive wall coupling.

The experimentally observed situation corresponds to chromaticity of about 15 units. Fig.5 shows that $l = 1$ mode is strongly unstable with the growth-time of about 40×10^{-3} sec, which would suggest that this mode is responsible for the observed betatron instability. One way of suppressing the $l = 1$ mode would be by decreasing chromaticity. This scheme has been successfully tried during the last fixed target run. However, as one can see from Fig.5, the $l = 0$ mode appears to be unstable for small positive chromaticities and might lead to significant enhancement of coherent betatron motion due to previously discussed resistive wall coupling. Fortunately, this potentially offending mode can be effectively suppressed by the active damper system also employed during the last fixed target run. This efficient cure for the $l = 0$ mode obviously does not work in case of the higher modes, since its feedback system picks up only the transverse position of a bunch centroid, which remains zero due to the symmetry of the higher modes. Another possible cure (also effective for the $l \geq 1$ modes) would involve the Landau damping through the octupole-induced betatron tune spread. Increasing betatron amplitude of initially unstable mode causes increase of the tune

spread , which will eventually self-stabilize development of this mode. The efficacy of this last scheme will be examined in the next fixed target run.

In conclusion, we identified observed coherent instability as a combination of the single bunch slow head-tail modes driven by the kicker magnets and the coupled bunch resistive wall instability. Good agreement between the measurements and the growth-times calculated within the framework of the presented model points strongly at the $l = 1$ mode as the offending single bunch component of the observed instability. Whether this picture is really true, or perhaps the $l = 0$ mode is present instead; this question should be addressed through a detailed high resolution real time observation carried out in the next run.

APPENDIX - EFFECTIVE IMPEDANCE CALCULATION

From the discussion of Section 4. we identified the kicker magnets as the offending contribution to the transverse coupling impedance which drives the head-tail instability in the Tevatron. The transverse coupling impedance is expressed analytically as follows

$$\text{Re } Z_{\perp}(\omega) = \frac{Z_0 L}{4ab} \frac{1}{\omega} \left(1 - \cos \frac{\omega L}{c} \right) \quad (\text{A.1})$$

We are only concerned with the real part of the impedance which enters into the growth-time formula, Eq(2.8) and (2.9). As mentioned before, $Z_{\perp}(\omega)$ has a diffraction-like character; a principle maximum of width $\lambda = \pi c/L$ at the origin and a series of equally spaced secondary maxima governed by the same width. Similarly the beam power spectrum harmonics, $\rho^l(\omega - \omega_k)$, have one ($l = 0$) or a pair ($l \geq 1$) of principle maxima of width $\varepsilon = \pi/2\hat{\tau}$ followed by a sequence of secondary maxima. Both spectra are sampled by a discrete set of frequencies given by

$$\omega_p = (p + v)\omega_0 \quad (\text{A.2})$$

In the limit of $\varepsilon, \lambda \ll \omega_0$ the variable ω_p gains continuous character on the scale of the structure of both functions. This allows to replace the infinite summation in Eq.(2.9) by the integration according to the following substitution

$$\sum_{p=-\infty}^{\infty} \dots \rightarrow \int_{-\infty}^{\infty} dp \dots \quad (\text{A.3})$$

Using specific impedance, given by Eq.(A.1) one can carry out the above integration and evaluate Z_{eff}^l in closed analytic form. First, one can simplify ρ^l , expressed by Eq.(2.4).

by applying the substitution defined by Eq.(A.3) to the sum in the denominator and integrating it explicitly. The resulting expression has the following form

$$\rho^\ell(\omega) = \frac{\hat{\tau}}{2\pi\omega_0} h_\ell(\omega)$$

where

(A.4)

$$h_\ell(\omega) = \frac{4}{\pi^2} (\ell + 1) \frac{1 + (-1)^\ell \cos(2\omega\hat{\tau})}{[(2\omega\hat{\tau}/\pi)^2 - (\ell + 1)^2]^2}$$

Substituting Eqs.(A.1) and (A.4) in Eq.(2.4) allows to rewrite the effective impedance in terms of the following integral

$$Z_{\text{eff}}^\ell = \frac{Z_0 c(\ell + 1)}{\omega_0 ab} \frac{\pi^2}{16} J^\ell$$

where

(A.5)

$$J^\ell = \int_{-\infty}^{\infty} d\omega \frac{[1 - \cos(\omega + \omega_\xi) \lambda] [1 + (-1)^\ell \cos(2\omega\hat{\tau})]}{(\omega + \omega_\xi)(\omega + \alpha)^2(\omega - \alpha)^2}$$

Here ω_ξ and $\alpha = \pi (\ell + 1)/2\hat{\tau}$ define poles in the complex ω -plane connected with chromatic phase shift and beam spectrum respectively. The integral J^ℓ can be expressed in terms of much simpler integrals defined by

$$J^+(t) = \int_{-\infty}^{\infty} d\omega \frac{\cos(\omega t)}{(\omega + \omega_\xi)(\omega + \alpha)^2(\omega - \alpha)^2}$$

(A.6)

$$J^-(t) = \int_{-\infty}^{\infty} d\omega \frac{\sin(\omega t)}{(\omega + \omega_\xi)(\omega + \alpha)^2(\omega - \alpha)^2} ,$$

in the following form

$$\begin{aligned} J &= J^+(0) + (-1)^\ell J^+(2\hat{t}) \\ &+ \cos(\omega_\xi \lambda) \left[(-1)^\ell \frac{J^+(\lambda + 2\hat{t}) + J^+(\lambda - 2\hat{t})}{2} - J^+(\lambda) \right] \\ &- \sin(\omega_\xi \lambda) \left[(-1)^\ell \frac{J^-(\lambda + 2\hat{t}) + J^-(\lambda - 2\hat{t})}{2} - J^-(\lambda) \right] \end{aligned} \quad (\text{A.7})$$

Both integrals given by Eq.(A.6) can be easily converted into contour integrals in the complex ω -plane and evaluated through Cauchy's theorem. The result is given below

$$\begin{aligned} J^+(t) &= \frac{\pi \sin \omega_\xi t}{(\omega_\xi^2 - \alpha^2)^2} - \frac{\pi \omega_\xi t}{2\alpha^2} \frac{\cos \alpha t}{\omega_\xi^2 - \alpha^2} + \frac{\pi \omega_\xi (\omega_\xi^2 - 3\alpha^2)}{2\alpha^3 (\omega_\xi^2 - \alpha^2)^2} \sin \alpha t \\ J^-(t) &= \frac{\pi \cos \omega_\xi t}{(\omega_\xi^2 - \alpha^2)^2} + \frac{\pi t \sin \alpha t}{2\alpha (\omega_\xi^2 - \alpha^2)} - \frac{\pi \cos \alpha t}{(\omega_\xi^2 - \alpha^2)^2} \end{aligned} \quad (\text{A.8})$$

Final substitution of Eqs.(A.5)–(A.8) into Eq.(2.4) leads after a tedious algebra to a simple closed formula describing the growth-time of the ℓ -th head-tail mode given below

$$\frac{1}{\tau^\ell} = \frac{ceI_0\beta}{4\pi\nu\gamma m_0} \frac{Z_0 R \pi^2}{ab} \frac{\pi(\ell+1)}{\chi^2 - \pi^2(\ell+1)^2} \times$$

$$\left[\frac{\chi}{2\pi^2(l+1)^2} + (-1)^l \frac{\sin\chi}{\chi^2 - \pi^2(l+1)^2} \right] \quad (\text{A.9})$$

Here $\chi = 2 \frac{v}{\eta} \omega_0 \hat{t}$, is the betatron phase shift between the head and tail of the bunch.

ACKNOWLEDGEMENT

We wish to thank Curtis Crawford for furnishing documentation on the Tevatron's kicker magnets.

REFERENCES

1. F. Sacherer, Proc. 9-th Int. Conf. on High Energy Accelerators, Stanford 1974, p. 347
2. F. Sacherer, CERN/SI-BR/72-5 (1972), unpublished
3. K.Y. Ng, Principles of the High Energy Hadron Colliders, Part I: The SSC, edited by A.W. Chao and M. Month
4. L.J. Laslett, V.K. Neil, A.M. Sessler, Rev. Sci. Instr., **36**, (1965), p. 436

FIGURE CAPTIONS

Fig. 1 Output from a beam position monitor showing the transverse beam position over 10 turns

Fig. 2 Real (a) and imaginary (b) part of the transverse coupling impedance of a unit bellow section (10 corrugations). Result of the TBCI simulation

Fig. 3 Harmonics of the beam power spectrum $\rho^2(\omega)$. Markers denote the sampling frequencies $\omega_p = \omega_0(Mp + n)$. Dimensionless frequency is given in units of $x = \frac{\omega}{M\omega_0}$

Fig. 4 Schematic diagram of the resistive wall coupled bunch instability combined with the slow head-tail $l = 1$ mode - suggested picture of the observed coherent betatron instability

Fig. 5 A family of inverse growth-time vs chromaticity curves evaluated numerically for various head-tail mode indices l

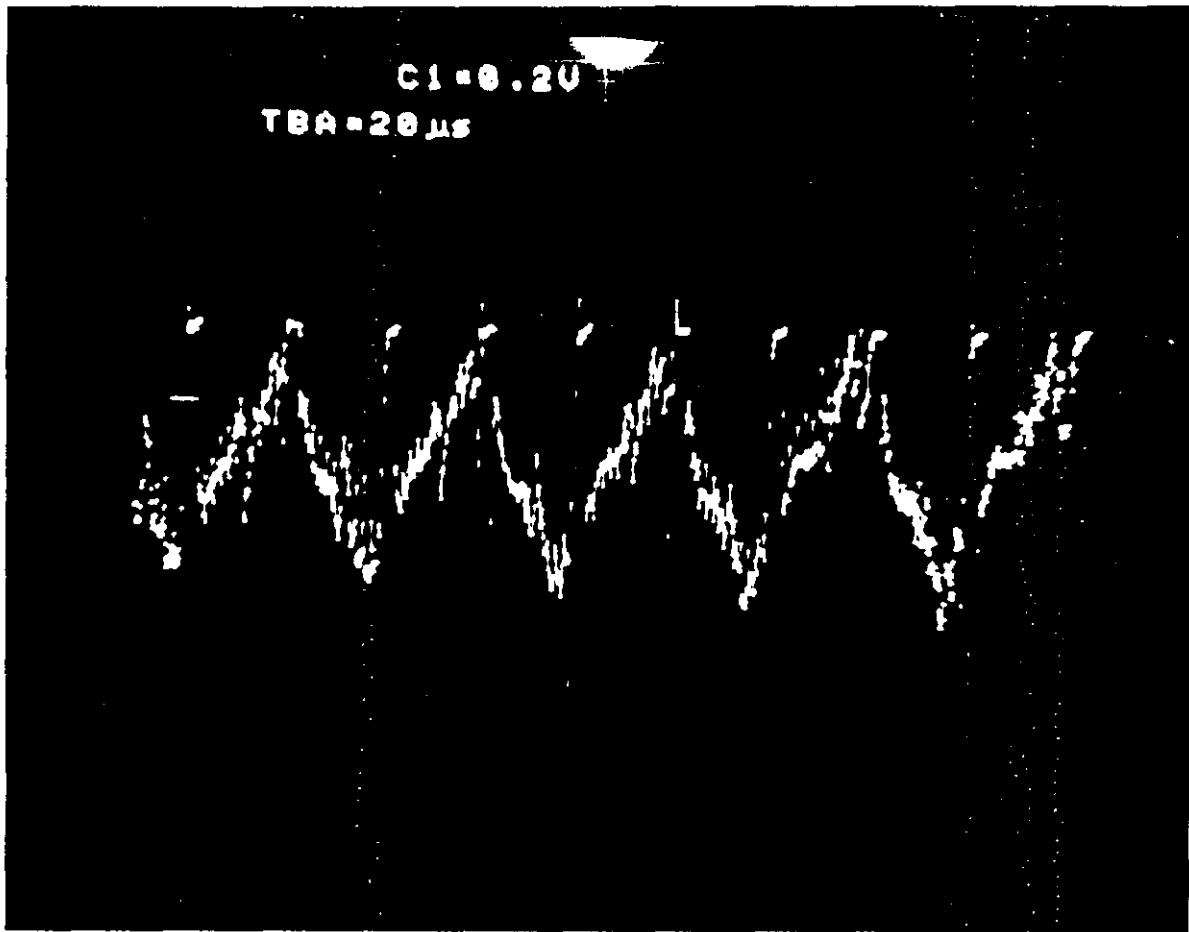


Fig. 1

TRANSVERSE IMPEDANCE (REAL)

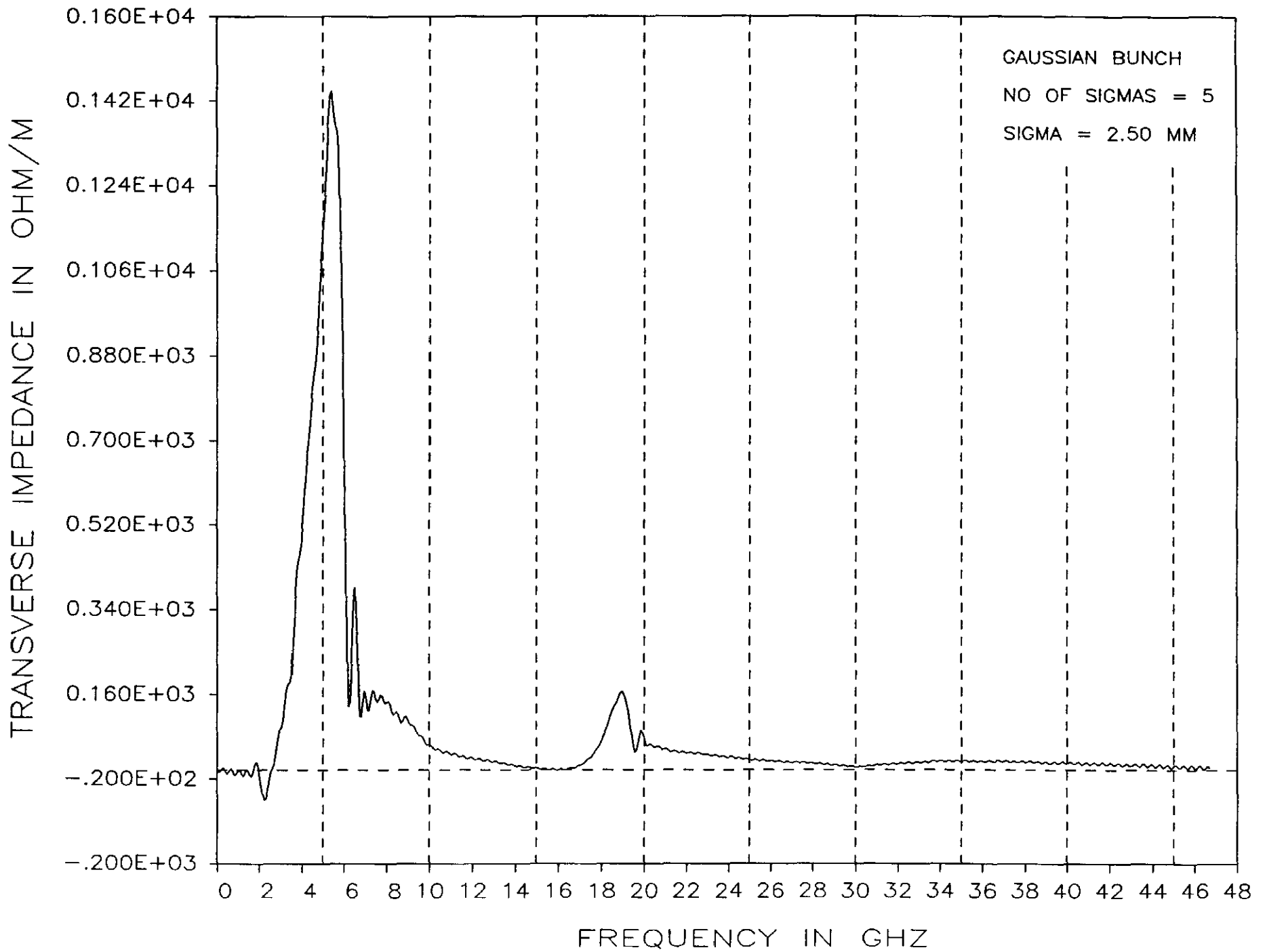


Fig. 2a

TRANSVERSE IMPEDANCE (IMAGINARY)

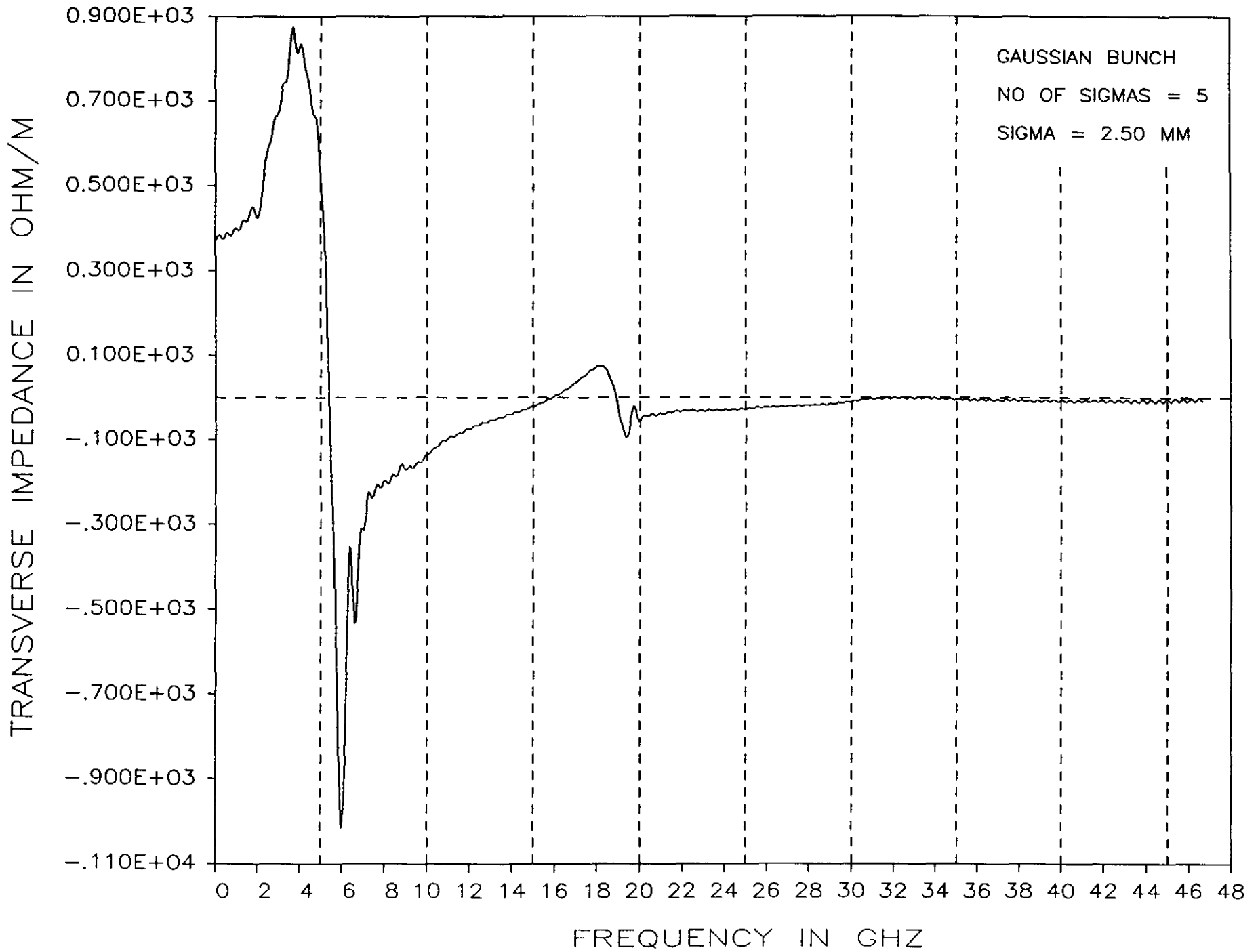


Fig. 2b

$\rho'(x)$

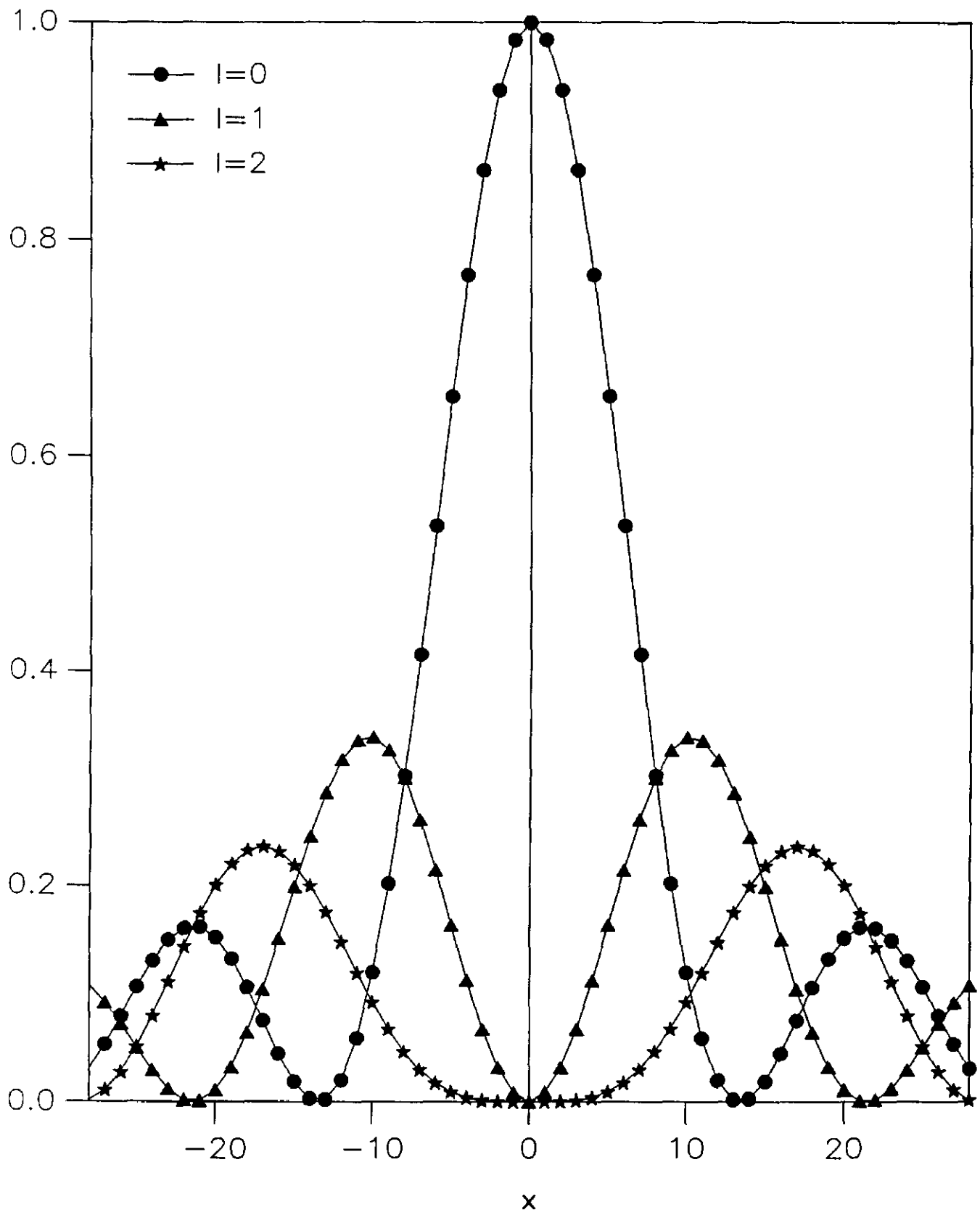


Fig. 3

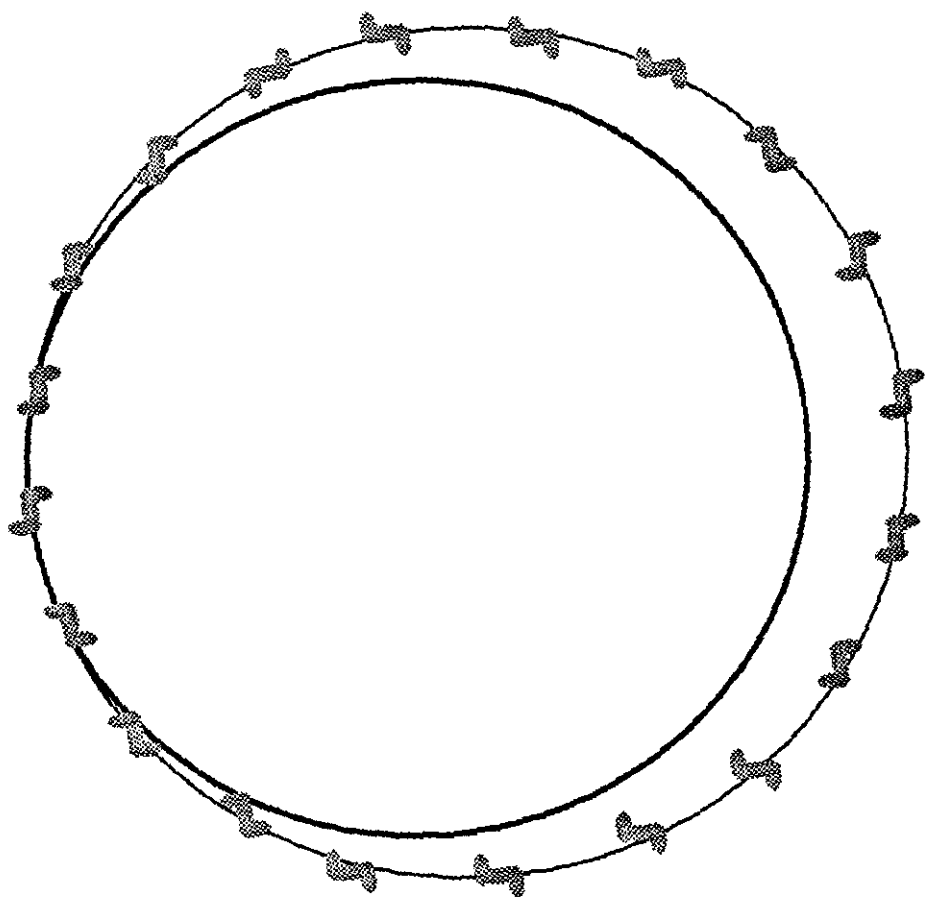


Fig. 4

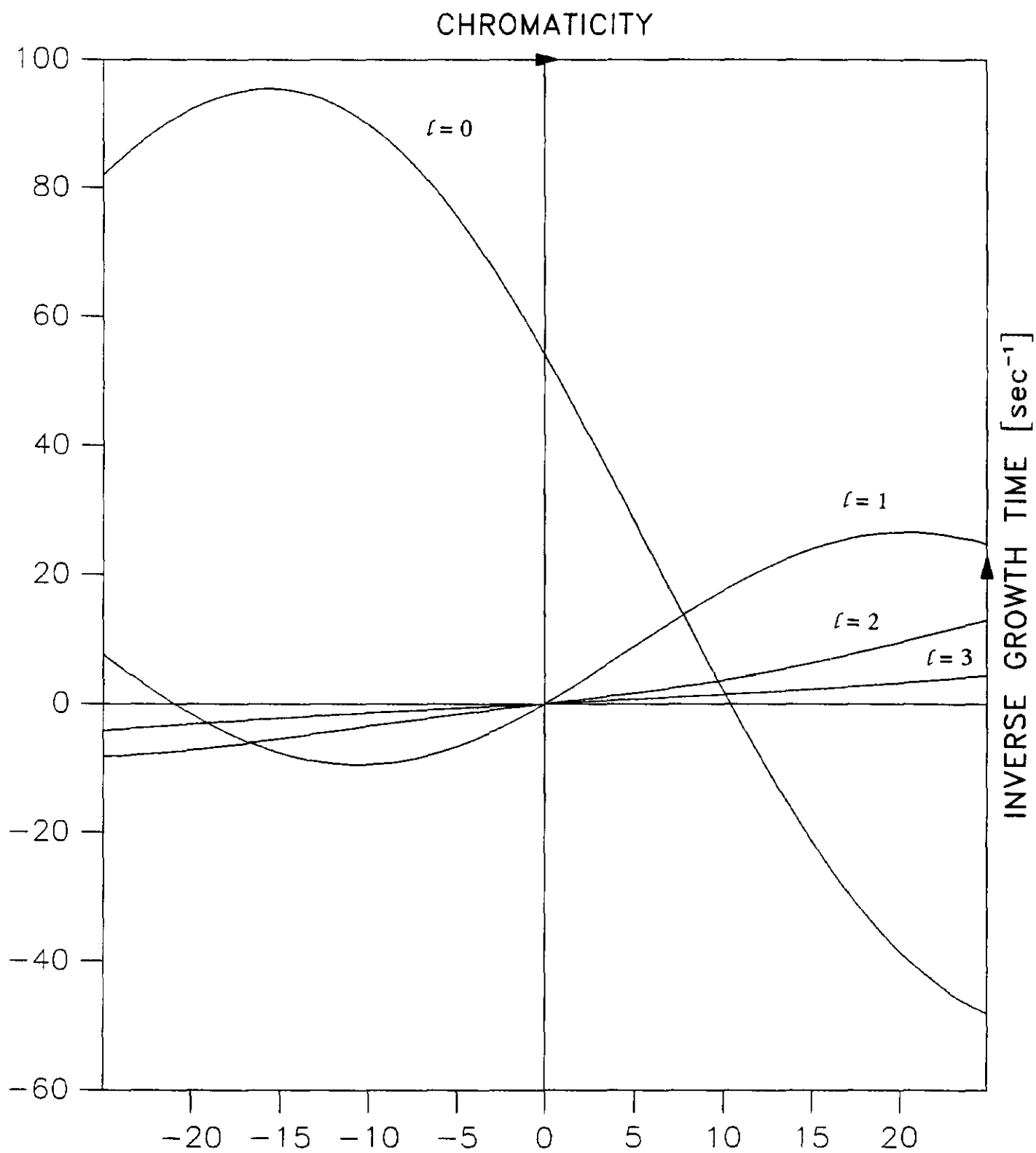


Fig. 5